

Photodissociation of multilayered trimethylaluminum adsorbed on a cryogenic substrate: a time-of-flight mass-spectrometric study

Makoto Kobayashi, Akihiko Sato, Yugo Tanaka, Hisanori Shinohara and Hiroyasu Sato*

Department of Chemistry for Materials, Faculty of Engineering, Mi'e University, Tsu 514, Japan

Photodissociation of trimethylaluminum [Al(CH₃)₃] adsorbed on a silica (SiO₂) substrate at 110 K has been studied by multiphoton ionization time-of-flight mass spectrometry. Translational energy distributions of aluminum and AlCH₃ fragments can be fitted with a composition of two Maxwell–Boltzmann distributions. The two components are attributed to different environments of photodissociating parent molecules in the multilayer.

Keywords: Organometallics, trimethylaluminum, photodissociation, time-of-flight mass spectrometry

1 INTRODUCTION

Alkyl metal compounds such as trimethylaluminum [Al(CH₃)₃] or trimethylgallium [Ga(CH₃)₃] have been frequently utilized in chemical vapor deposition (CVD) processes for the micro dry processes of semiconductors. There are a variety of CVD methods presently available. In particular, the photo-CVD method attracts wide interest because selective photoexcitations of various organometallics can be achieved by using visible and UV lasers. For example, UV excimer lasers have been used as the dissociation light source in many investigations; for reviews, see (for example) Refs 1–5. Higashi⁶ studied UV (193 nm) photodissociation of Al(CH₃)₃ on oxide (Al₂O₃, SiO₂ or SiO₂/Si) substrates at room temperature. He detected methyl radicals by a quadrupole mass spectrometer, and found that the kinetic energy associated with methyl radicals was only 25 meV, a surprisingly small amount compared

with the available energy (3.5 eV). Effective dissipation of excitation energy to the surface was indicated. Zhang and Stuke⁷ studied photodissociation (at 308, 248 and 193 nm) processes of trimethyl-, triethyl-, and tri-isobutyl-aluminum (AlR₃) adsorbed on a silicon and/or quartz substrate at room temperature. The major aluminum-containing products detected were aluminum atoms and AlH and AlCH₃ fragments. The velocity distributions of Al⁺ and AlCH₃⁺ did not fit to the Maxwell–Boltzmann (MB) distribution. Orłowski and Mantell⁸ detected CH₃ and Al(CH₃)_n (*n* = 1, 2, 3) species by laser photodissociation (193 nm) of Al(CH₃)₃ adsorbed on aluminum-coated silicon and SiO₂ substrates at room temperature. The obtained time-of-flight data of the fragments were fitted to the MB distributions. In addition they have observed AlH₂ fragments upon photodissociation. In the present study, multiphoton ionization time-of-flight mass spectrometry was applied to study the photodissociation of Al(CH₃)₃ adsorbed on a cryogenic quartz substrate. Translational energy distributions of the photofragments (Al and AlCH₃) are reported, and the photodissociation mechanism is discussed.

2 EXPERIMENTAL

The experimental apparatus for multiphoton ionization (MPI)/time-of-flight (TOF) mass-spectrometric measurements is shown schematically in Fig. 1. The vacuum chamber was evacuated with a 6-in (15-cm) diffusion pump (1400 l s⁻¹) backed up by a rotary pump. Pressure in the chamber was maintained below 2×10^{-6} Torr when a sample gas was introduced. Trimethylaluminum [Al(CH₃)₃] was purchased from Aldrich. Since Al(CH₃)₃ has a low vapor

* To whom correspondence should be addressed.

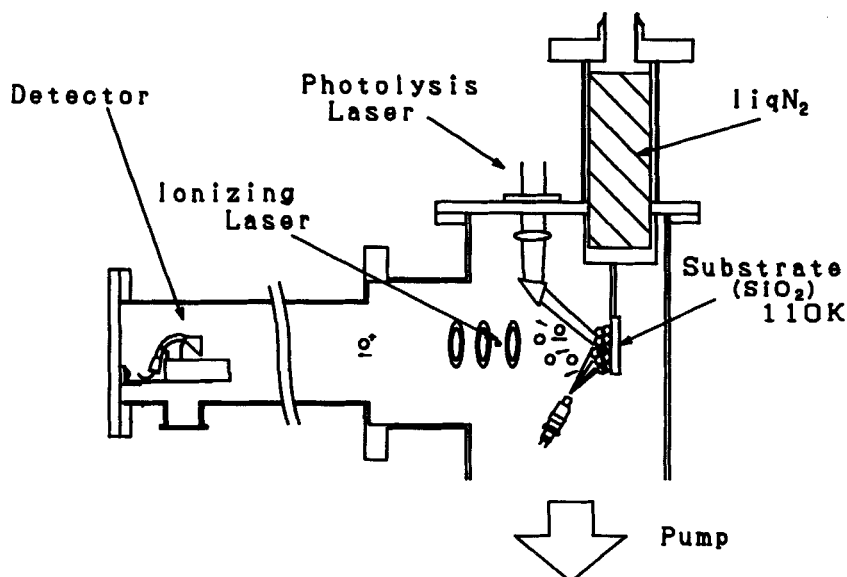


Figure 1 A schematic view of the apparatus for multiphoton ionization TOF mass-spectroscopic measurements.

pressure (20 Torr at 297 K), seeded sample gas was prepared by bubbling helium gas through liquid $\text{Al}(\text{CH}_3)_3$.

A quartz (SiO_2) substrate in the chamber was cooled to approx. 110 K by liquid nitrogen. The sample gas was injected onto the quartz substrate through an electric fuel injector (duration approx. 0.5 ms, 2 Hz). $\text{Al}(\text{CH}_3)_3$ molecules are dimerized on the cooled substrate at 110 K.

An ArF excimer laser (Lambda Physik LPX-100) was used as a photodissociation light source. The laser light was focused by a quartz lens ($f=200$ mm) on the substrate. Typically the laser flux on the substrate was 30 mJ cm^{-2} . Photodissociated fragments were desorbed and entered the ionizing region of the TOF mass spectrometer, where they were ionized with a dye laser (Lambda Physik FL-3000) pumped by a XeCl excimer laser LPX-100. The laser wavelength between 440 and 450 nm was selected by using Coumarin 440 dye. Dye laser pulses (~ 10 mJ) were focused into the ionization region in the chamber by a quartz lens ($f=300$ mm). The ions were detected by a home-made TOF mass spectrometer (a 50 cm drift region) equipped with a Channeltron ion detector (Galileo). The ion signal was amplified by an HP-4900 preamplifier and fed to a Lecroy 9400A digital oscilloscope (typical sampling time was 10 ns). The data were analyzed by a microcomputer (NEC PC-9801). All timings were controlled by a

home-made sequence controller. By varying the time delay between the desorption and the ionization lasers, one can obtain the TOF distribution of a particular fragment.

3 RESULTS AND DISCUSSION

3.1 Observed photofragments

Resonance-enhanced multiphoton ionization (REMPI)/TOF mass-spectrometric measurements of photofragments of $\text{Al}(\text{CH}_3)_3$ were performed at several wavelengths at which effective ionization of observed fragments (Al , AlCH_3 and AlH) can be achieved.

A typical TOF mass spectrum of the photofragments is shown in Fig. 2. The spectrum was averaged over 100 times. It was confirmed that there were no background signals due to residual vapor samples. The delay time between the dissociation and the ionization laser pulses was $\sim 22 \mu\text{s}$. Two distinct peaks were observed in Fig. 2 at mass numbers of 27 and 42, corresponding to aluminum (Al^+) and monomethylaluminum (AlCH_3^+) ions, respectively. The relative intensity of these TOF signals was found to change drastically with the dye laser wavelength. In Fig. 2 the dye laser was tuned to excite the $\text{C}^1\text{A}_1 \leftarrow \text{X}^1\text{A}_1$ transition of AlCH_3 (22624 cm^{-1}).⁷ When the wavelength of the dye laser was chosen so as to

excite the $C^1A_1 \leftarrow X^1A_1$ transition of AlH (22306 cm^{-1})⁹ (Fig. 3), a peak corresponding to AlH^+ was observed in addition. Furthermore, the intensity of the $AlCH_3^+$ ion decreased relative to that of Al^+ . In the gas phase $Al(CH_3)_3$ exists in the dimerized state, i.e. as $Al_2(CH_3)_6$, at room temperature.¹⁰ Neither dimer ion $Al_2(CH_3)_6^+$ nor monomer ion $Al(CH_3)_3^+$ has been observed in our experiment. The dimerization energy of $Al(CH_3)_3$ is rather low (0.87 eV) and the dimer is easily photodissociated. $Al(CH_3)_3$ has predissociative states near 6 eV.¹¹ Formation of metal hydride molecules has been reported for several organometallic molecules.¹² Because $Al(CH_3)_3$ has no β -hydrogen atom, the AlH radical cannot be produced from isolated $Al(CH_3)_3$ by a β -hydrogen elimination mechanism. AlH is most probably formed on the substrate surface when a parent molecule is excited, by abstracting a hydrogen atom from a neighboring $Al(CH_3)_3$ molecule.

3.2 Origin of observed ions

Figure 4 shows the dye laser wavelength dependence of Al^+ and $AlCH_3^+$ peak intensities in the observed mass spectra. Four peaks found for the Al^+ signal can be assigned to the two photon transitions of the aluminum atom¹³ ($7p\ ^2P_{1/2}(J=\frac{1}{2})$ or $\frac{3}{2}) \leftarrow 3p\ ^2P_{1/2}(J=\frac{1}{2})$ or $\frac{3}{2})$ and $6f\ ^2F_{1/2}(J=\frac{5}{2})$ or $\frac{7}{2}) \leftarrow 3p\ ^2P_{1/2}(J=\frac{1}{2})$ or $\frac{3}{2})$). This shows that the MPI process involves resonance absorption of neutral aluminum atoms. Therefore, the Al^+ signal is due to MPI of neutral aluminum atoms. $AlCH_3^+$ shows a broad peak around 442 nm. It is close to the position where Zhang and Stuke⁹ found a peak in

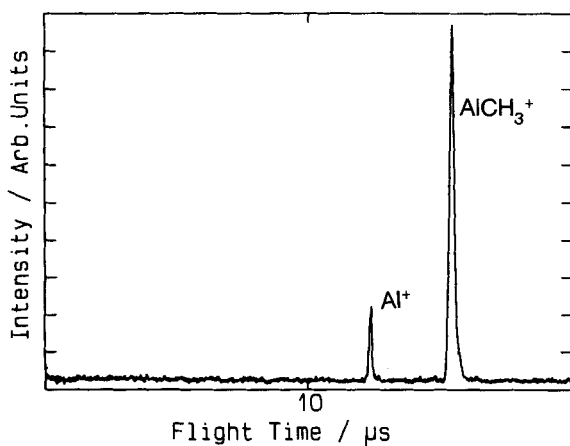


Figure 2 A TOF mass spectrum of trimethylaluminum on a SiO_2 substrate at 110 K photodissociated by the ArF 193 nm excimer laser. Dye laser wavelength: 442.0 nm.

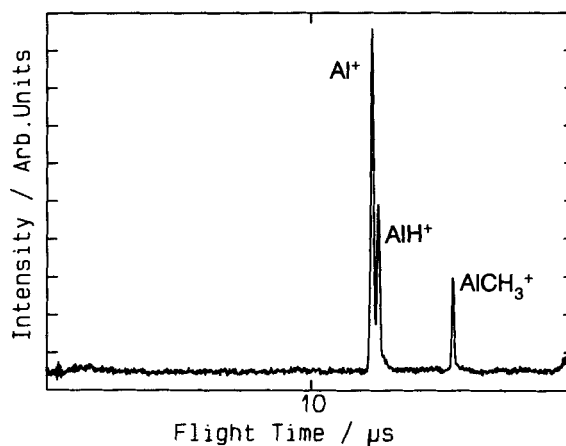


Figure 3 A TOF mass spectrum of trimethylaluminum on a SiO_2 substrate at 110 K photodissociated by the ArF 193 nm excimer laser. Dye laser wavelength: 448.5 nm.

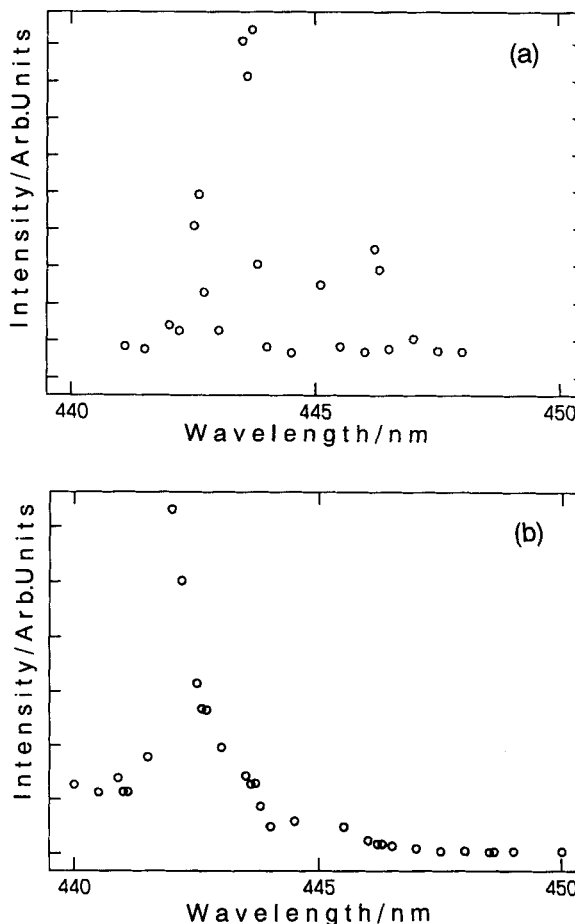


Figure 4 Dye laser wavelength dependence of the intensity of (a) Al^+ and (b) $AlCH_3^+$.

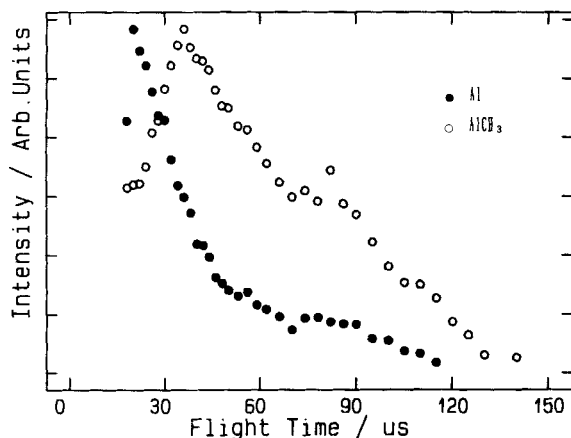


Figure 5 TOF distributions of neutral fragments aluminum and AlCH_3 from a SiO_2 substrate. The flight length is 2.8 cm.

the photodissociation of gas-phase and surface-adsorbed $\text{Al}(\text{CH}_3)_3$. They assigned this band to the electronic transition ($\bar{C}^1\text{A}_1 \leftarrow \bar{X}^1\text{A}_1$) of neutral AlCH_3 .⁷ Therefore, the AlCH_3^+ signal in our experiment can be assigned to the MPI of neutral AlCH_3 , although the possibility that it is due to the MPI of some larger fragment(s) such as $\text{Al}(\text{CH}_3)_2$ cannot be totally ruled out, since the absorption spectrum of $\text{Al}(\text{CH}_3)_2$ is not known. Not shown in the figure is the dye laser wavelength dependence of the AIH intensity which exhibits a narrow band at 448.5 nm.

3.3 Kinetic energy distributions of neutral fragments

By monitoring the intensity of the ion signal with the variation of the delay time between dissociation and ionization laser pulses, the TOF distribution (from the substrate surface to the ionization region) of the neutral fragment corresponding to the observed ion was measured. Figure 5 shows the results of such TOF measurements on Al^+ and AlCH_3^+ ions. Apparently the two distributions are different. This finding excludes the possibility that two ions stem from a common neutral precursor. In other words, this confirms that they are from different neutral precursors. These are assigned to Al and AlCH_3 , respectively (Section 3.2 above). The TOF spectra are converted to the translational energy distribution by Eqn [1]:

$$P(E_T) = CI(t)^2/ml^2 \quad [1]$$

where $I(t)$ is the TOF signal intensity, t is the flight time, m is the mass of the fragment, l is the

flight length, and C is a normalization constant. Figure 6 shows the translational energy distribution spectrum so obtained for aluminum atoms. It cannot be fitted with a single Maxwell-Boltzmann (MB) distribution. When it is fitted as a sum of two MB components as shown in the figure, the translational temperatures of the two components are $T_1(\text{trans}) = 160$ K and $T_2(\text{trans}) = 1400$ K. Figure 7 is the translational energy distribution spectrum of AlCH_3 fragments extracted from the same set of TOF data as for the aluminum distribution. It can again be fitted with a sum of two MB components, $T_1(\text{trans}) = 190$ K and $T_2(\text{trans}) = 1000$ K.

Zhang and Stuke⁷ studied TOF distributions of aluminum and AlCH_3 from photodissociation of $\text{Al}(\text{CH}_3)_3$ on n-Si(100) and SiO_2 surfaces. The peak translational energy was 0.069 eV for aluminum and 0.017 eV for AlCH_3 . They compared the velocity distribution of aluminum with a MB distribution ($T = 1100$ K). The experimental distribution was much broader than the MB distribution, and it was characterized with a long tail of higher-velocity component. Zhang and Stuke mentioned that the fast component was due to 'photodissociation', although it was not discussed further. Orlowski and Mantell⁸ studied photodissociation of $\text{Al}(\text{CH}_3)_3$ on the aluminum-covered SiO_2/Si surface. Although they found no evidence for desorption of aluminum atoms from the surface, larger aluminum-containing species were detected. They all corresponded with single MB distributions ($T = 388$ K for $\text{Al}(\text{CH}_3)_3$, $T = 920$ K for $\text{Al}(\text{CH}_3)_2$, $T = 1290$ K for AlCH_3 , and $T = 990$ K for CH_3). No evidence for desorption of aluminum was ascribed by these authors, as indi-

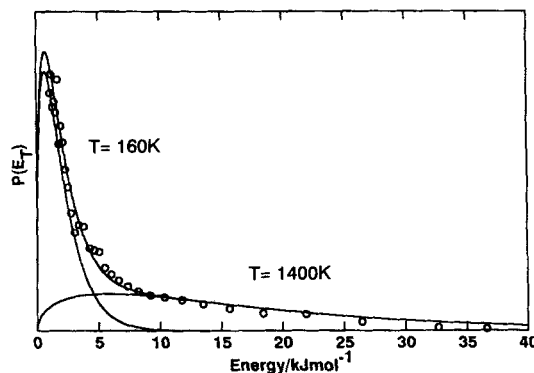


Figure 6 Translational energy distribution of an aluminum atom. Circles indicate experimental values. The three curves show single MB distributions ($T = 160$ K and $T = 1400$ K) and their sum, respectively.

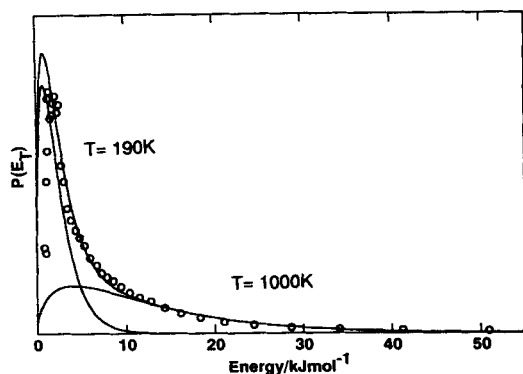


Figure 7 Translational energy distribution of AlCH_3 radical. Circles indicate experimental values. The three curves show single MB distributions ($T = 190$ K and $T = 1000$ K) and their sum, respectively.

cating that aluminum is more tightly bound to the surface than methylaluminum fragments. The translational temperature of the fast component of AlCH_3 in our experiments (1290 K) is quite close to theirs. However, our results show the presence of a slower component in addition. Higashi⁶ measured the translational energy distribution of methyl radicals from $\text{Al}(\text{CH}_3)_3$ photodissociated by a 193 nm laser. The distribution was found to correspond with a MB distribution of $T = 150$ K. No other fragment was detected. Because we did not observe CH_3^+ ions, no direct comparison can be made between these results and ours. However, Higashi's observation of a very low translational temperature species has some parallel to the presence of the low-temperature component in our results.

The greatest point of difference between our experimental conditions and those of Zhang and Stuke,⁷ Orlowski and Mantell⁸ and Higashi⁶ is the temperature of the substrate. In their experimental conditions, the substrate was maintained at room temperature and the sample was adsorbed in less than one monolayer (1 ML) on the substrate. In our experimental conditions, the substrate was cooled by liquid nitrogen and parent molecules adsorbed in a multilayer. Observation of two components in our case must be due to adsorption in a multilayer.

Observation of a translational energy distribution with multiple components has been reported. van Veen *et al.*¹⁴ studied TOF distribution for laser etching of CuCl . The distribution was fitted with two contributions: a MB and a Gaussian distribution. They attributed the MB part to a one-photon process and the Gaussian part to a

multiphoton process. In our experiment the translational energy distribution of aluminum atoms was composed of two MB components. It suggests that at least two paths exist for their creation. Several explanations can be conceived for the bimodal distribution. First, aluminum atoms corresponding to the slower component may be created from photodissociation of some larger fragment(s) after desorption. That is to say, some fragment(s) larger than an aluminum atom was desorbed from the surface, and the fragment(s) absorb another photon in the same laser pulse to dissociate to give an aluminum atom. This possibility can be excluded because the laser pulse width (~ 10 ns) is much shorter than the flight time of fragments (in the order of $10 \mu\text{s}$). Second, some thermalization by collisions may occur in the vapor phase immediately after dissociation. However, since the two fragments, Al and AlCH_3 , we observed show different temperatures, the possibility of collisional thermalization in nascent vapor is small. Therefore, the two components must correspond to different amounts of kinetic energy of aluminum atoms when they were ejected from the surface. The higher- and lower-temperature components are given by a dissociation-desorption process yielding a larger and smaller energy transferable into kinetic energy, respectively. Such a difference may be explained, among other ways, by variation of the environments of parent molecules at the photodissociation events. The parent $\text{Al}(\text{CH}_3)_3$ molecules of higher-temperature aluminum atoms suffer low energy loss. The parent molecules are probably those physisorbed on or very close to the surface of the multilayer. When it absorbs a UV photon, the parent molecule is dissociated and much excess energy is transferred into the translational energy of the fragments (aluminum atoms) as a result of low-energy dissipation. Aluminum atoms due to this process are ejected from the surface directly and give the fast TOF component.

Motooka *et al.* proposed¹⁵ that $\text{Al}(\text{CH}_3)_3$ dimer in the vapor phase photodissociates in a cascade single-photon absorption process. One photon is needed for the dissociation of dimer and a photon is needed for breaking each $\text{Al}-\text{CH}_3$ bond. Callender *et al.*¹⁶ measured the translational energy distributions of Al^+ ions from visible (456.2 nm) photodissociation of $\text{Al}(\text{CH}_3)_3$ in a supersonic jet. The translational distribution was approximately MB and the translational temperature was 1800 K. They attributed the distribution

to a combination of sequential dissociations. If aluminum atom formation from the photodissociation of $\text{Al}(\text{CH}_3)_3$ dimer on the solid substrate occurs as in the vapor phase, four photons must be necessary. However, there should exist some energy dissipation process through the surface. Therefore excess energy which is available for the translational energy will be reduced, and/or a further photon may be necessary to create an aluminum atom on the surface.

Recently Beuermann and Stuke¹⁷ showed that $\text{Al}(\text{CH}_3)_3$ can dissociate to $\text{AlCH}_3 + 2\text{CH}_3$ with one photon ($<220\text{ nm}$) in the vapor phase. If this path is the major one in the adsorbed phase, generation of two aluminum atoms from $\text{Al}(\text{CH}_3)_3$ dimer requires five photons. The average Al–C bond energy for $\text{Al}(\text{CH}_3)_3$ is approx. 2.9 eV,¹⁸ and the dimerization energy is 0.87 eV, where 1 eV = 96.5 kJ mol⁻¹.¹⁹ If it is assumed that five photons at 193 nm (6.4 eV) are required for formation of two aluminum atoms from $\text{Al}_2(\text{CH}_3)_6$, then in total approx. 13.8 eV of excess energy is available. If the equipartition law is assumed, the mean translational energy is calculated as 0.27 eV, corresponding to a translational temperature of 2100 K. Some dissipation of energy to the substrate may reduce the amount of translational energy eventually left with the desorbing aluminum atoms ($T = 1400\text{ K}$).

The average kinetic energy of the lower-temperature component ($\frac{3}{2}kT = 0.02\text{ eV}$) seems too low to be a result of the direct dissociation mechanism. The component must correspond to the fragments which lose a large amount of excess energy before the desorption. It is suggested that energy equilibration (or exchange) exists between the slow aluminum atom and the surface of the substrate.

The result of translational distribution analysis of the AlCH_3 fragment is similar to the case of the aluminum atom: the distribution can be fitted with the sum of two MB distributions, and each component has a temperature comparable to that of the aluminum atoms. An explanation similar to the case of the aluminum atoms could be made, although more information is required for a quantitative discussion on the comparison of translational energy distributions of aluminum and AlCH_3 .

Chuang and Domen²⁰ studied the electronically excited photodissociation of CH_2I_2 molecules on Al_2O_3 and aluminum surfaces at 308 nm. The signal intensity maximum of the CH_2I photo-fragment TOF spectra changed according to the

surface coverage of CH_2I_2 (parent) molecules. When the surface coverage increased to a multilayer ($\theta > 15$), the peak translational distribution energy increased significantly from $E_T = 0.095\text{ eV}$ at $\theta \leq 1$ to $\sim 1\text{ eV}$ at $\theta = 30$. They proposed an explosive desorption regime for such observations. No evidence for such a process was found in our case.

4 CONCLUSION

Photodissociation of trimethylaluminum [$\text{Al}(\text{CH}_3)_3$] adsorbed on a SiO_2 substrate at 110 K has been studied by multiphoton ionization time-of-flight mass spectrometry. Translational energy distributions of aluminum and AlCH_3 fragments can be fitted with a composition of two Maxwell–Boltzmann distributions. The two components are attributed to different environments of photodissociating parent molecules in the multilayer.

Acknowledgements The authors thank Mr H. Nakamura for his assistance.

REFERENCES

1. Ehrlich, D J and Tsao, J Y *Vac. Sci. Technol.*, 1983, B1: 969
2. Osgood, R M, Jr *Ann. Rev. Phys. Chem.*, 1983, 34: 77
3. Yardley, J T In *Laser Handbook*, vol 5, Stich, M L (ed), North-Holland, Amsterdam, 1985, pp 405–454
4. Sato, H (ed) *Appl. Organomet. Chem.*, 1991, 5: 207–348
5. Sato, H. In *Progress in Photochemistry and Photophysics*, vol 6, Rabek, J F (ed), CRC Press, Boca Raton, 1992, pp 135–166
6. Higashi, G S *J. Chem. Phys.*, 1985, 88: 422
7. Zhang, Y and Stuke M *J. Phys. Chem.*, 1989, 93: 4503
8. Orłowski, T E and Mantell, D A *J. Vac. Sci. Technol.*, 1989, A7: 2598
9. Zhang, Y and Stuke, M *Chem. Phys. Lett.*, 1989, 149: 310
10. Beuermann, Th and Stuke, M *Appl. Phys.*, 1989, B49: 145
11. Motooka, T, Gorbatskin, S, Lubben, D, Eres D and Greene, J E *J. Vac. Sci. Technol.*, 1986, A4: 3146
12. Zhang, Y and Stuke, M *J. Cryst. Growth*, 1988, 93: 143
13. Mitchell, S A and Hackett, P A *J. Chem. Phys.*, 1983, 79: 4815
14. van Veen, G N A, Baller, T and de Vries, A E *J. Appl. Phys.*, 1986, 60: 3746

15. Motooka, T, Gorbalkin, S, Lubben, D, Eres D and Greene, J E J. *Appl. Phys.*, 1985, 58: 4397
16. Callendar, C L, Rayner, D M and Hackett, P A *Appl. Phys.*, 1988, B47: 7
17. Beuermann, Th and Stuke, M *Chem. Phys. Lett.*, 1991, 178: 197
18. Chem. Soc. Jpn. (ed.), Kagaku Benran, Maruzen, Tokyo, 1984
19. Laubengayer, A W and Gilman, W F J. *Am. Chem. Soc.*, 1941, 63: 477
20. Chuang, T J and Domen, K J. *Vac. Sci. Technol.*, 1987, A5: 4732